Organometallics 1993, 12, 1616–1622

Fluxional Behavior of the σ,π-Vinyl Complexes $\mathrm{Os_2\{\mu\text{-}CH{=}C(H)Ph\}(\mu\text{-}Br)(CO)_{6-n}(PPh_3)_n}$ (n = 1, 2): Use of $^{13}C\{^1H\}$ NOE and ^{187}Os–^{13}C Couplings in Assignment of Carbonyls

Louis J. Farrugia*

Department of Chemistry, University of Glasgow, Glasgow G12 8QQ, Scotland, U.K.

Yun Chi and Wen-Cheng Tu

Department of Chemistry, National Tsing Hua University, Hsinchu 30043, Taiwan

Received December 28, 1992

The fluxional behavior of the complexes $\mathrm{Os_2\{\mu\text{-}CH{=}C(H)Ph\}(\mu\text{-}Br)(CO)_{6-n}(PPh_3)_n}$ (**1**, n = 1; **2**, n = 2) has been examined quantitatively by ^{13}C and ^{31}P 1D magnetization transfer and 2D EXSY measurements. Complex **1**, which exists in solution as the two isomers **1a** and **1b**, shows three independent exchange processes at 273 K: tripodal rotations of the $Os(CO)_3$ groups in the major isomer **1a** ($k = 5.18\ s^{-1}$) and minor isomer **1b** ($k = 0.25\ s^{-1}$) and a σ,π-vinyl flip leading to the interconversion of **1a** and **1b** ($k = 2.37\ s^{-1}$). Complex **2** in solution shows a single exchange process, a σ,π-vinyl flip with $k = 0.53\ s^{-1}$ at 265 K. Crystal data for **2**: monoclinic, space group $P2_1/c$, a = 14.256(1) Å, b = 11.650(1) Å, c = 25.841(2) Å, β = 90.243(5)°, V = 4291.9(5) Å^3, R (R_w) = 0.030 (0.032) for 6231 independent absorption-corrected data to θ = 26°. Couplings to ^{187}Os were observed for both complexes, and these were used in conjunction with $^{13}C\{^1H\}$ NOE and ^{13}C DQF-COSY experiments to provide unambiguous assignments of all carbonyl resonances.

Introduction

Detailed studies on the dynamic behavior of hydrocarbyl ligands on clusters[1] may provide information about the energetics and mobility of organic molecules on metal surfaces. The fluxional behavior of one such ligand, σ,π-vinyl, was first reported in 1975 by Shapley and co-workers[2] in the cluster $\mathrm{Os_3(\mu\text{-}H)(\mu\text{-}CH{=}CH_2)(CO)_{10}}$. A number of other μ-vinyl complexes with similar dynamic behavior were subsequently reported.[3–14] In the σ,π-vinyl flip mechanism, the μ-$CR_1{=}CR_2R_3$ ligand formally shifts the π- and σ-bonds between the metal atoms. The reported NMR spectra of the complexes $\mathrm{[Mo_2(\mu\text{-}CH{=}CH_2)(CO)_4Cp_2]^+(BF_4)^-}$[7] and $\mathrm{[Fe_2(\mu\text{-}PhC{=}CH_2)(CO)_6(dppm)](BF_4)^-}$[14] suggest that the geminal CH_2 protons undergo exchange during the σ,π-vinyl flip. In all other cases the chemical distinction between the substituents R_2 and R_3 is maintained during the vinyl flip.

Recently one of us has reported[15] the synthesis and variable-temperature ^1H and ^{13}C NMR spectra of the vinyl complexes $\mathrm{Os_2\{\mu\text{-}CH{=}C(H)Ph\}(\mu\text{-}Br)(CO)_{6-n}(PPh_3)_n}$ (**1**; n = 1) and (**2**; n = 2). Complex **1** exists in solution as two isomers, which undergo exchange on the NMR time scale. Although it was proposed that this behavior was due to a σ,π-vinyl flip, the possibility of a tripodal rotation of the $Os(CO)_2(PPh_3)$ group was also suggested. The reported activation barriers $\Delta G^{\ddagger}$ for both the σ,π-vinyl flip mechanism (41–53 kJ mol^{-1})[2–4,8] and tripodal rotation of $M(CO)_2(PR_3)$ groups (48–66 kJ mol^{-1})[16–18] have similar values. In fact, both mechanisms are entirely consistent with the NMR data. A tripodal rotation of the $Os(CO)_2(PPh_3)$ group, within the isomer of **1** observed in the crystal structure,[15] cannot per se result in equivalence of the two carbonyls, since they are diastereotopic, but it will generate a second isomer. Since the structures of the isomers of **1** were not ascertained, and ^{13}C signals for the carbonyls were not assigned,[15] there remained some doubt as to the exact exchange mechanism.

Herein we report further NMR studies on complexes **1** and **2**. These studies demonstrate the successful use of

---

[1] (a) Band, E.; Muetterties, E. L. *Chem. Rev.* **1978**, *78*, 639. (b) Johnson, B. F. G.; Benfield, R. E. In *Transition Metal Clusters*; Johnson, B. F. G. Ed.; Wiley: New York, 1980.

[2] (a) Keister, J. B.; Shapley, J. R. *J. Organomet. Chem.* **1975**, *85*, C29. (b) Shapley, J. R.; Richter, S. I.; Tachikawa, M.; Keister, J. B. *J. Organomet. Chem.* **1975**, *94*, C43.

[3] Clauss, A. D.; Tachikawa, M.; Shapley, J. R.; Pierpont, C. G. *Inorg. Chem.* **1981**, *20*, 1528.

[4] (a) Nubel, P. O.; Brown, T. L. *J. Am. Chem. Soc.* **1984**, *106*, 644. (b) Nubel, P. O.; Brown, T. L. *J. Am. Chem. Soc.* **1984**, *106*, 3474. (c) Lee, K.-W.; Brown, T. L. *Organometalics* **1985**, *4*, 1030.

[5] Aime, S.; Gobetto, R.; Osella, D.; Milone, L.; Rosenberg, E.; Anslyn, E. V. *Inorg. Chim. Acta* **1986**, *111*, 95.

[6] Bassner, S.; Morrison, E. D.; Geoffroy, G. L. *Organometallics* **1987**, *6*, 2207.

[7] Beck, J. A.; Knox, S. A. R.; Riding, G. H.; Taylor, G. E.; Winter, M. J. *J. Organomet. Chem.* **1980**, *202*, C49.

[8] Dyke, A. F.; Knox, S. A. R.; Morris, M. J.; Naish, P. J. *J. Chem. Soc., Dalton Trans.* **1983**, 1417.

[9] Gerlach, R. F.; Duffy, D. N.; Curtis, M. D. *Organometallics* **1983**, *2*, 1172.

[10] Green, M.; Orpen, A. G.; Schaverien, C. J. *J. Chem. Soc., Dalton Trans.* **1989**, 1333.

[11] Xue, Z.; Sieber, W. J.; Knobler, C. B.; Kaesz, H. D. *J. Am. Chem. Soc.* **1990**, *112*, 1825.

[12] Fryzuk, M. D.; Jones, T.; Einstein, F. W. B. *Organometallics* **1983**, *3*, 185.

[13] Burch, R. R.; Shusterman, A. J.; Muetteries, E. L.; Teller, R. G.; Williams, J. M. *J. Am. Chem. Soc.* **1983**, *105*, 3546.

[14] Boothman, J.; Hogarth, G. *J. Organomet. Chem.* **1992**, *437*, 201.

[15] Chuang, S.-H.; Chi, Y.; Liao, F.-L.; Wang, S.-L.; Peng, S.-M.; Lee, G.-H.; Wu, J.-C.; Horng, K.-M. *J. Organomet. Chem.* **1991**, *410*, 85.

[16] (a) Rosenberg, E.; Thornsen, C. B.; Milone, L.; Aime, S. *Inorg. Chem.* **1985**, *24*, 231. (b) Jangala, C.; Rosenberg, E.; Skinner, D.; Aime, S.; Milone, L.; Sappa, E. *Inorg. Chem.* **1980**, *19*, 1571. (c) Aime, S.; Gobetto, R.; Osella, D.; Milone, L.; Rosenberg, E. *Organometallics* **1982**, *1*, 640. (d) Rosenberg, E.; Bracker-Novak, J.; Gellert, R. W.; Aime, S.; Gobetto, R.; Osella, D. *J. Organomet. Chem.* **1989**, *365*, 163.

[17] Farrugia, L. J.; Rae, S. *Organometallics* **1992**, *11*, 196.

[18] Alex, R. F.; Pomeroy, R. K. *J. Organomet. Chem.* **1985**, *284*, 379.

0276-7333/93/2312-1616$04.00/0 © 1993 American Chemical Society

Chart I

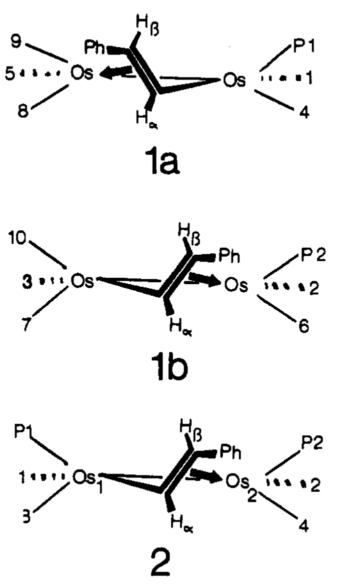

the $^{13}C\{^1H\}$ NOE and ^{187}Os–^{13}C and ^{13}C–^{13}C J couplings in the unambiguous assignment of the carbonyl resonances and also confirm that a σ,π-vinyl flip is occurring in both complexes. These methods of carbonyl assignment are preferable to those based on chemical shifts, which are inherently unreliable.

Table I. ^{13}C NMR Parameters for Complexes 1 and 2

reson[a]	chem shift, ppm[b]	J, Hz[c]		
		Os–C	P–C	C–C
		Complex 1		
1 (**1a**)	189.3	93	3.5	3.8
2 (**1b**)	183.6	116	2.7	4.9, 0.5
3 (**1b**)	181.2	90	1.7	3.3, 0.4
4 (**1a**)	180.6	145	5.8	3.8
5 (**1a**)	179.3	118	2.1	4.1, 0.2
6 (**1b**)	177.5	141	4.1	4.9
7 (**1b**)	176.6	141	0.3	3.3, 3.3
8 (**1a**)	174.3	135	1.1	2.8, 4.1
9 (**1a**)	173.8	125	1.4	2.8, 0.2
10 (**1b**)	173.1	127	1.3	3.3, 0.4, 0.5
C_α (**1a**)	144.7			
C_α (**1b**)	144.1			
C_β (**1b**)	81.7			
C_β (**1a**)	81.0			
		Complex 2		
1	190.9	93	2.8, 1.6	3.7
2	185.7	118	1.7, 1.7	4.9
3	182.3	144	5.5, ~0.2	3.7
4	179.3	139	4.1, 1.1	4.9
C_α	146.0			
C_β	80.2			

[a] For assignments see Chart I. [b] CD_2Cl_2, 243 K. [c] Coupling constants: C–C and P–C, ±0.1 Hz; Os–C ±1 Hz.

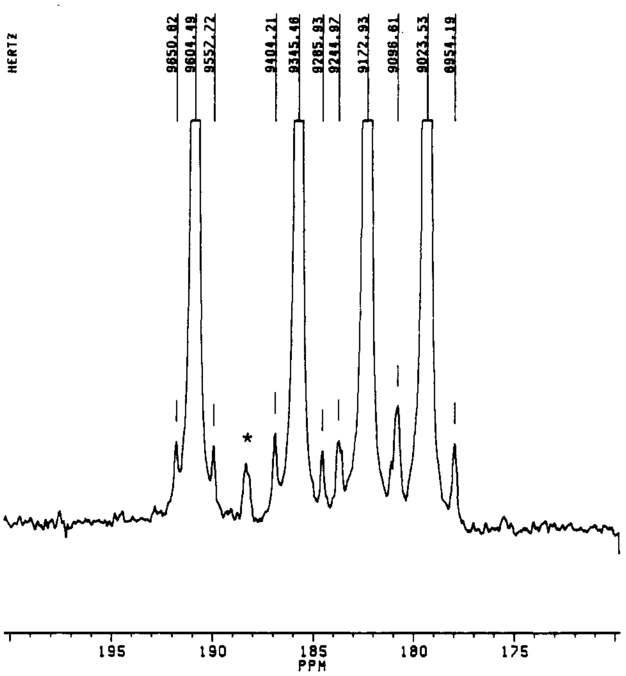

Figure 1. ^{13}C NMR spectrum of complex **2** in the carbonyl region, showing the ^{187}Os satellites. The peak marked with an asterisk (*) is due to an impurity.

Results and Discussion

Fluxional Behavior and X-ray Structure of 2. The NMR spectra of complex **2**, which exists as one detectable isomer in solution, will be discussed first. As previously reported,[15] the ^{13}C spectrum shows four equally intense signals in the carbonyl region, given in Table I. With the high level of ^{13}C enrichment (~65%), the ^{187}Os satellites are clearly observable (see Figure 1), and the magnitudes of $^1J(^{187}Os–^{13}C)$ are given in Table I. A ^{13}C EXSY spectrum (265 K, mixing time t_m = 0.5 s) showed that the high-frequency resonances 1 and 2 were exchanging with each other, as were the low-frequency signals 3 and 4. This is consistent with the reported variable-temperature study.[15] The exchange rate constants $k_{12} = 0.54 \pm 0.06\ s^{-1}$ and $k_{34} = 0.52 \pm 0.06\ s^{-1}$ were obtained from a kinetic analysis of the EXSY intensities by the method of Abel et al.[19] This method assumes that the cross relaxation rates σ_{ij} are negligible in comparison with the exchange rates. Hawkes et al.[20] have shown that, even with high levels of ^{13}C enrichment, the measured value of σ_{CC} in $Os_3(\mu\text{-}H)_2(CO)_{10}$ is insignificant (~$10^{-4}\ s^{-1}$).

The ^{31}P NMR spectrum of **2** shows two equally intense doublets at δ 15.2 and −1.8. A ^{31}P EXSY spectrum at 265 K showed these two signals were exchanging, and the rate constant $k_{PP} = 0.53 \pm 0.04\ s^{-1}$ was obtained from analysis of the EXSY intensities. ^{13}C and ^{31}P EXSY spectra were also measured at the higher temperature of 299 K and gave rate constants $k_{12} = 25.4 \pm 2.8\ s^{-1}$, $k_{34} = 31.5 \pm 3.5\ s^{-1}$, and $k_{PP} = 27.1 \pm 2.8\ s^{-1}$. A value for k_{PP} of 30.4 s^{-1} (299 K) was also obtained from a 1D ^{31}P magnetization transfer experiment at 299 K, using a DANTE pulse train to selectively invert P(1). Clearly, at both temperatures, all three rate constants k_{12}, k_{34}, and k_{PP} are identical within experimental error. This indicates that a single mechanism must be responsible for the observed exchanges and also indicates that the ^{31}P–^{31}P cross-relaxation rate σ_{PP} must be small.

When discussing fluxional mechanisms, it is helpful to be as certain as possible of the structures in solution, in order to obtain entirely unambiguous assignments. The ^{31}P chemical shifts of **2** in solution are very similar to the isotropic shifts of δ 19.4 and −0.9 obtained from a ^{31}P CPMAS spectrum of a crystalline sample of **2**. This implies that the same structure is maintained in both phases. The ligand geometry of **2** in the solid state was determined by a single-crystal X-ray study. Final positional parameters

---

(19) Abel, E. W.; Coston, T. P. J.; Orrell, K. G.; Sik, V.; Stephenson, D. *J. Magn. Reson.* **1986**, *70*, 34.

(20) Hawkes, G. E.; Randall, E. W.; Aime, S.; Osella, D.; Elliot, J. E. *J. Chem. Soc., Dalton Trans.* **1984**, 279.

Table II. Fractional Coordinates and Displacement Parameters (Å²)

	x	*y*	*z*	U^a
Os(1)	0.21647(2)	0.18637(2)	−0.11520(1)	0.034
Os(2)	0.33989(2)	0.00543(2)	−0.11946(1)	0.033
Br	0.16378(4)	−0.02254(5)	−0.09393(2)	0.041
P(1)	0.07055(10)	0.26616(12)	−0.13570(5)	0.036
P(2)	0.38248(10)	−0.19073(12)	−0.12172(5)	0.034
O(11)	0.3338(3)	0.3901(4)	−0.1431(2)	0.078
O(12)	0.2044(4)	0.2502(5)	−0.0006(2)	0.086
O(21)	0.5290(3)	0.0914(4)	−0.1510(2)	0.076
O(22)	0.3958(4)	0.0639(5)	−0.0090(2)	0.089
C(1)	0.2720(4)	0.1122(4)	−0.1820(2)	0.035
C(2)	0.2686(4)	−0.0004(4)	−0.2004(2)	0.034
C(11)	0.2872(4)	0.3135(5)	−0.1316(2)	0.048
C(12)	0.2070(4)	0.2270(5)	−0.0440(3)	0.053
C(21)	0.4561(5)	0.0568(5)	−0.1392(2)	0.048
C(22)	0.3745(5)	0.0397(5)	−0.0504(3)	0.054
C(101)	0.3158(5)	−0.0384(3)	−0.2495(2)	0.035
C(102)	0.4001(5)	0.0092(5)	−0.2664(2)	0.050
C(103)	0.4414(3)	−0.0304(4)	−0.3119(1)	0.058
C(104)	0.3986(4)	−0.1177(3)	−0.3404(2)	0.062
C(105)	0.3143(4)	−0.1654(5)	−0.3234(1)	0.063
C(106)	0.2729(2)	−0.1257(4)	−0.2780(2)	0.046
C(111)	0.0499(4)	0.2911(6)	−0.2052(1)	0.038
C(112)	0.0029(5)	0.3876(3)	−0.2240(2)	0.047
C(113)	−0.0107(3)	0.4015(4)	−0.2771(2)	0.059
C(114)	0.0229(3)	0.3188(5)	−0.3115(1)	0.059
C(115)	0.0699(4)	0.2223(3)	−0.2927(2)	0.053
C(116)	0.0835(3)	0.2085(5)	−0.2395(3)	0.047
C(121)	−0.0272(3)	0.1734(4)	−0.1161(1)	0.041
C(122)	−0.0301(4)	0.1406(6)	−0.0643(2)	0.058
C(123)	−0.1026(4)	0.0703(5)	−0.0466(1)	0.069
C(124)	−0.1721(3)	0.0329(3)	−0.0808(1)	0.069
C(125)	−0.1691(4)	0.0658(6)	−0.1327(2)	0.064
C(126)	−0.0967(3)	0.1359(5)	−0.1504(1)	0.049
C(131)	0.0379(6)	0.4021(3)	−0.1042(3)	0.040
C(132)	−0.0564(5)	0.4327(5)	−0.1004(1)	0.062
C(133)	−0.0815(3)	0.5358(5)	−0.0768(3)	0.076
C(134)	−0.0122(5)	0.6083(3)	−0.0569(2)	0.073
C(135)	0.0821(4)	0.5777(5)	−0.0607(2)	0.069
C(136)	0.1072(4)	0.4746(5)	−0.0843(3)	0.056
C(211)	0.3212(5)	−0.2822(5)	−0.1690(1)	0.033
C(212)	0.3666(2)	−0.3400(4)	−0.2090(2)	0.048
C(213)	0.3163(4)	−0.4154(2)	−0.2406(2)	0.056
C(214)	0.2208(4)	−0.4329(4)	−0.2323(1)	0.056
C(215)	0.1754(2)	−0.3750(3)	−0.1923(2)	0.051
C(216)	0.2256(5)	−0.2997(3)	−0.1606(2)	0.046
C(221)	0.3625(3)	−0.2778(5)	−0.0633(2)	0.044
C(222)	0.3842(6)	−0.3945(4)	−0.0650(2)	0.063
C(223)	0.3689(5)	−0.4634(3)	−0.0216(3)	0.080
C(224)	0.3319(3)	−0.4154(4)	0.0233(2)	0.088
C(225)	0.3102(6)	−0.2987(3)	0.0250(2)	0.096
C(226)	0.3255(5)	−0.2299(4)	−0.0183(3)	0.070
C(231)	0.5066(3)	−0.2099(5)	−0.1353(3)	0.042
C(232)	0.5397(3)	−0.1794(7)	−0.1841(3)	0.058
C(233)	0.6352(4)	−0.1876(5)	−0.1950(2)	0.081
C(234)	0.6977(3)	−0.2263(5)	−0.1571(3)	0.118
C(235)	0.6645(3)	−0.2569(6)	−0.1083(3)	0.115
C(236)	0.5690(4)	−0.2486(4)	−0.0974(2)	0.068
H(1)	0.32010	0.16310	−0.19820	0.080
H(2)	0.21320	−0.05130	−0.18950	0.080

[a] For hydrogen atoms *U* is the isotropic displacement parameter, and for other atoms $U = {}^1/_3\sum_{i=1}^{3}\sum_{j=1}^{3}U_{ij}a^*_ia_j(\vec{a}_i\cdot\vec{a}_j)$.

Table III. Selected Bond Lengths (Å) and Angles (deg)

Os(1)–Os(2)	2.748(1)	Os(1)–Br	2.606(1)
Os(1)–P(1)	2.337(2)	Os(1)–C(1)	2.090(6)
Os(1)–C(11)	1.841(7)	Os(1)–C(12)	1.905(7)
Os(2)–Br	2.619(1)	Os(2)–P(2)	2.365(2)
Os(2)–C(1)	2.255(6)	Os(2)–C(2)	2.323(5)
Os(2)–C(21)	1.835(7)	Os(2)–C(22)	1.893(7)
O(11)–C(11)	1.154(8)	O(12)–C(12)	1.154(9)
O(21)–C(21)	1.158(8)	O(22)–C(22)	1.145(9)
C(1)–C(2)	1.396(7)	C(2)–C(101)	1.504(8)

Os(2)–Os(1)–Br	58.5(1)	Os(2)–Os(1)–P(1)	149.9(1)
Os(2)–Os(1)–C(1)	53.5(2)	Os(2)–Os(1)–C(11)	104.9(2)
Os(2)–Os(1)–C(12)	106.1(2)	Br–Os(1)–P(1)	99.3(1)
Br–Os(1)–C(1)	84.2(2)	Br–Os(1)–C(11)	163.3(2)
Br–Os(1)–C(12)	90.4(2)	P(1)–Os(1)–C(1)	108.5(2)
P(1)–Os(1)–C(11)	96.6(2)	P(1)–Os(1)–C(12)	93.0(2)
C(1)–Os(1)–C(11)	86.2(3)	C(1)–Os(1)–C(12)	158.4(3)
C(11)–Os(1)–C(12)	93.6(3)	Os(1)–Os(2)–Br	58.0(1)
Os(1)–Os(2)–P(2)	155.0(1)	Os(1)–Os(2)–C(1)	48.1(2)
Os(1)–Os(2)–C(2)	77.3(2)	Os(1)–Os(2)–C(21)	109.9(2)
Os(1)–Os(2)–C(22)	88.0(2)	Br–Os(2)–P(2)	97.6(1)
Br–Os(2)–C(1)	80.8(2)	Br–Os(2)–C(2)	78.9(2)
Br–Os(2)–C(21)	167.9(2)	Br–Os(2)–C(22)	92.0(2)
P(2)–Os(2)–C(1)	128.7(2)	P(2)–Os(2)–C(2)	93.5(2)
P(2)–Os(2)–C(21)	94.4(2)	P(2)–Os(2)–C(22)	99.3(2)
C(1)–Os(2)–C(2)	35.5(2)	C(1)–Os(2)–C(21)	90.4(3)
C(1)–Os(2)–C(22)	132.0(3)	C(2)–Os(2)–C(21)	98.7(3)
C(2)–Os(2)–C(22)	165.2(3)	C(21)–Os(2)–C(22)	87.8(3)
Os(1)–Br–Os(2)	63.5(1)	Os(1)–C(1)–Os(2)	78.4(2)
Os(1)–C(1)–C(2)	131.1(4)	Os(2)–C(1)–C(2)	75.0(3)
Os(2)–C(2)–C(1)	69.6(3)	Os(2)–C(2)–C(101)	124.9(4)
C(1)–C(2)–C(101)	123.3(5)	Os(1)–C(11)–O(11)	177.1(6)
Os(1)–C(12)–O(12)	177.6(6)	Os(2)–C(21)–O(21)	178.5(6)
Os(2)–C(22)–O(22)	177.8(6)		

are given in Table II and selected metrical parameters in Table III. The molecular structure shown in Figure 2 reveals that both phosphine ligands are coordinated cis to the μ-Br group and are in "equatorial" sites relative to the Os_2Br triangle. Most of the metrical parameters for **2** closely resemble those reported for **1**[15] and call for little comment. However, the two Os–Br separations in **2** differ by only 0.013 Å, compared with 0.061 Å in **1**, although in both cases the shorter distance is to the Os atom which is formally σ-bonded to the vinyl group.

In order to aid assignment of the ^{13}C resonances, a ^{13}C-{^1H} NOE difference experiment (253 K) was undertaken. Irradiation of the H_α proton (H(1)) at δ 8.81 resulted in NOE's of ~5% at the low-frequency CO resonances at δ 182.3 and 179.3, while irradiation of the H_β proton [H(2)] at δ 3.55 produced no detectable NOE's at any CO resonance (see Figure 3). This indicates that the two low-frequency CO resonances 3 and 4 are due to the "equatorial" CO's proximal to H_α (C(11) and C(21) in Figure 2). In order to determine which pairs of CO's were attached to the same Os atom, a ^{13}C DQF-COSY spectrum was obtained. This showed that the pairs of resonances (1,3) and (2,4) form separate spin systems, with mutual couplings of 3.7 and 4.9 Hz, respectively. It has been established that there is a small cis coupling of ~2–4 Hz between carbonyls in $M(CO)_3$ groups,[21] so that resonances 1 and 3 belong to one $Os(CO)_2(PPh_3)$ group and resonances 2 and 4 to the other. These data, together with the EXSY spectra, uniquely characterize the exchange process in **2** as a σ,π-vinyl flip, which results in a time-averaged molecular mirror plane. From the mean of the rate constants at 253 K, we estimate $\Delta G^{\ddagger}_{253}$ = 66.0 (±0.6) kJ mol^{-1}.

The ^{13}C and ^{31}P NMR signals for **2** could be assigned to individual $Os(CO)_2(PPh_3)$ groups by comparison with the data obtained for complex **1** below. The solid-state structure[15] of **1b** shows that the phosphine is attached to the Os atom which is formally π-bonded to the vinyl ligand, while the CPMAS ^{31}P spectrum for **1b** shows an isotropic shift at δ −3.3. A comparison with the solid-state and solution ^{31}P chemical shifts for **2** clearly implies that the phosphorus atom P(2), attached to the osmium atom Os(2) in **2**, which is formally π-bonded to the vinyl group and

---

[21] (a) Aime, S.; Osella, D. *J. Chem. Soc., Chem. Commun.* **1981**, 300. (b) Hawkes, G. E.; Lian, L. Y.; Randall, E. W.; Sales, K. D. *J. Chem. Soc., Dalton Trans.* **1985**, 225.

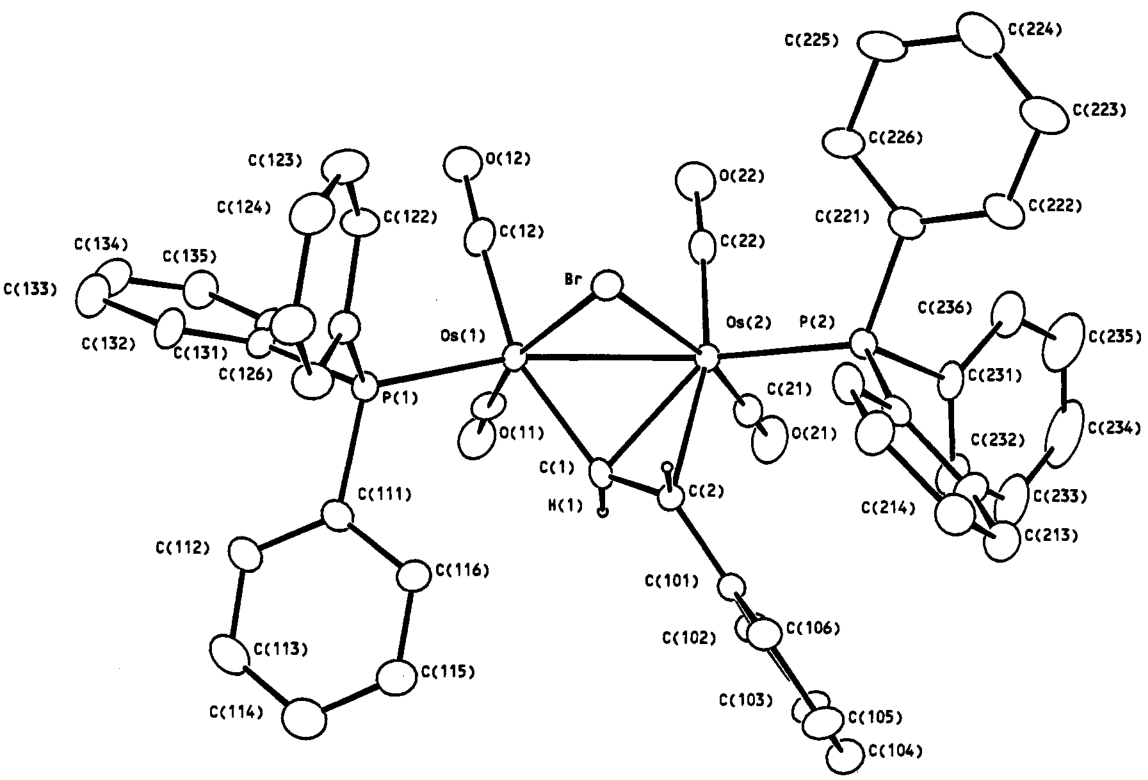

Figure 2. Molecular structure and atomic labeling scheme for complex 2. Thermal ellipsoids are drawn at the 20% probability level; hydrogen atoms are shown as spheres of arbitrary radius.

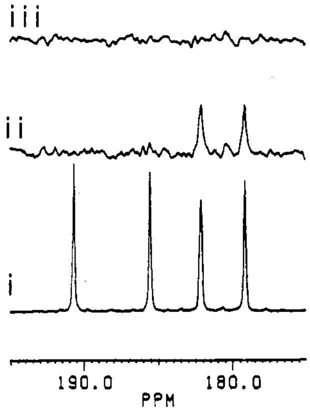

Figure 3. $^{13}C\{^1H\}$ NOE difference spectra for complex 2: (i) control off-resonance spectrum; (ii) irradiation at H_α minus control spectrum; (iii) irradiation at H_β minus control spectrum.

which is in a chemical environment similar to that for the phosphine in **1b**, must give rise to the most shielded solution resonance at δ −1.8.

The carbonyl resonances 1 and 2 in complex **2** have significantly different magnitudes of 93 and 118 Hz for $J(^{187}Os-^{13}C)$. The latter is identical, within error, to that found for signal 2 in complex **1b** (see Table I). This signal may be unambiguously assigned to the CO ligand in the $Os(CO)_2(PPh_3)$ group which lies trans to the π-bond of the vinyl group. Hence, the assignment of resonances 1 and 2 in **2** to the carbonyls C(12) and C(22) (see Figure 2) and resonances 3 and 4 to C(11) and C(21) follows. The magnitudes of $J(^{187}Os-^{13}C)$ have been reported for a number of osmium carbonyl compounds,[22-27] and it is apparent that they are sensitive to stereo geometry. For instance, in clusters containing the $Os(CO)_4$ group, the axial CO ligands have values of $J(^{187}Os-^{13}C)$ in the range 84–90 Hz, while for the equatorial CO ligands this range is 115–123 Hz.[22]

Finally, it appears that the vinyl flip mechanism in **2** may also operate in the solid state. A ^{31}P experiment (ambient temperature, t_m = 5.0 s) using the 2D pulse sequence of Szeverenyi et al.,[28] which corresponds to a solid-state EXSY experiment, showed strong cross peaks between the isotropic shifts, indicative of either chemical exchange or spin diffusion due to $^{31}P-^{31}P$ cross relaxation. This interesting process is under further investigation.

Fluxional Behavior of 1. Complex **1** exists in solution as two isomers[15] and exhibits resonances of unequal intensity at δ 17.5 and −0.8 in the ^{31}P NMR spectrum, due respectively to isomers **1a** and **1b**. At 263 K the equilibrium constant K for the reaction **1a** ↔ **1b** is 0.66, and this rises to 1.02 at 193 K. This indicates that the isomerization **1a** → **1b** is exothermic, and from the temperature dependence of K we estimate $\Delta H = -3.7\ (\pm 0.5)$ kJ mol^{-1} and $\Delta S = -17.6\ (\pm 1.9)$ J mol^{-1} K^{-1}. A crystalline sample of **1** shows a single isotropic shift of δ −3.3 in the ^{31}P CPMAS spectrum, indicating that isomer **1b**, with the *higher* free energy in solution at ambient temperature, corresponds to the solid-state structure.

The variable-temperature ^{13}C spectrum of **1** has been discussed.[15] Ten resonances (signals 1–10, Table I) are observed in the CO region, due to the five inequivalent carbonyls of both isomers. Satellites arising from ^{187}Os

---

[22] Farrugia, L. J. *J. Organomet. Chem.* **1990**, *394*, 515.

[23] Ewing, P.; Farrugia, L. J.; Rycroft, D. S. *Organometallics* **1988**, 7, 859.

[24] Koridze, A. A.; Kizas, O. A. *Organomet. Chem. USSR* **1989**, *2*, 87; *Metalloorg. Khim.* **1989**, *2*, 165.

[25] Koridze, A. A.; Kizas, O. A.; Astakhova, N. M.; Petrovskii, P. V.; Grishin, Yu. K. *J. Chem. Soc., Chem. Commun.* **1981**, 853.

[26] Gallop, M. A.; Johnson, B. F. G.; Lewis, J. *J. Chem. Soc., Chem. Commun.* **1987**, 1831.

[27] Gallop, M. A.; Johnson, B. F. G.; Khattar, R.; Lewis, J.; Raithby, P. R. *J. Organomet. Chem.* **1990**, *386*, 121.

[28] Szeverenyi, N. M.; Sullivan, M. J.; Maciel, G. E. *J. Magn. Reson.* **1982**, *47*, 462.

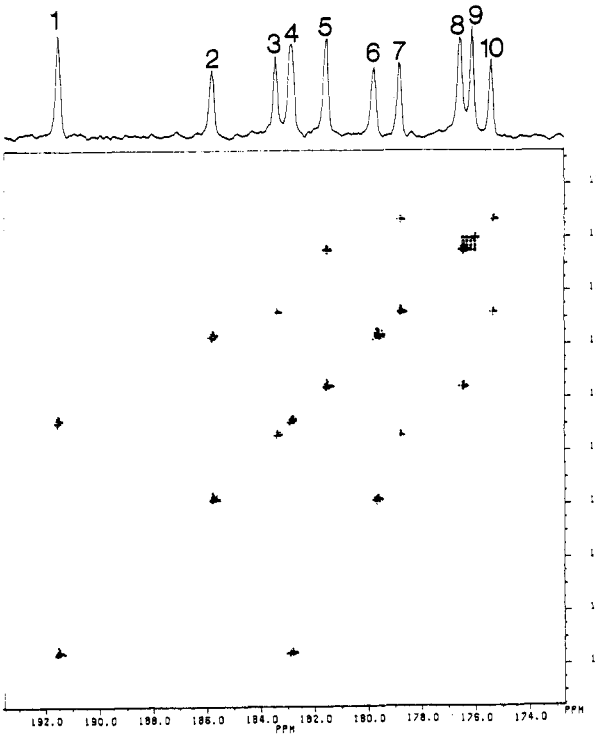

Figure 4. ^{13}C DQF-COSY (50.3 MHz) spectrum of complex 1 at 243 K.

coupling are clearly distinguished for all CO signals in the spectrum recorded at 150.9 MHz. Individual signals are readily ascribed to each isomer on the basis of intensity. Since resonances 1, 4 and 2, 6 show the largest ^{31}P couplings, they are assigned to the $Os(CO)_2(PPh_3)$ groups of isomers **1a** and **1b**, respectively. Signals 5, 8, and 9 may then be assigned to the $Os(CO)_3$ group of **1a** and signals 3, 7, and 10 to the same group in **1b**. This assignment was confirmed by a ^{13}C DQF-COSY spectrum (Figure 4), which showed the sets of resonances (1,4), (2,6), (3,7,10), and (5,8,9) formed separate spin systems. The coupling constants, given in Table I, were obtained from examination of the multiplet structure of each resonance, which was complicated by the presence of several isotopomers. The coupling constants between the pairs of resonances (3,10) and (5,9) are very small and do not appear in the DQF-COSY spectrum. In fact, the most abundant isotopomer for the $Os(CO)_3$ groups, which is the triply ^{13}C labeled species, does not contribute to the COSY spectrum because of the double quantum filter. The only coupling observed between carbonyls on different Os atoms was a small coupling (J = 0.5 Hz) between resonance 2 and resonance 10.

Further assignments depend on the interpretation of the structure of isomer **1a**. Possible structures are shown in Chart II. Structure A corresponds to a vinyl flip from **1b**, structures D and E correspond to a tripodal rotation of the $Os(CO)_2(PPh_3)$ group from **1b**, and structures B and C correspond to a combination of both processes. Structures C–E can be ruled out on the basis of $^{13}C\{^1H\}$ NOE experiments at 245 K. Figure 5 shows the carbonyl NOE's resulting from irradiation at three proton sites: (ii) the accidentally degenerate H_α protons of isomers **1a** and **1b** at δ 8.95, (iii) the H_β proton of **1a** at δ 4.40, and (iv) the H_β proton of **1b** at δ 3.75. In the case of (ii) there are significant NOE's for resonances 4 (6%), 6 (4.5%), 7 (7%), and 8 (4%). On the basis of the known structure of **1b**,[15] resonances 2, 6, 7 may be unambiguously assigned from this result. This experiment also indicates that isomer **1a** has two "equatorial" CO ligands lying close to H_α, which eliminates structures C and E. There are weak relayed NOE's at resonances 5 (0.5%) and 9 (1%) due to the tripodal rotation of the $Os(CO)_3$ group (see below), which occurs because the irradiation time of 4 s is significant compared to the exchange lifetime (~5 s). In addition, a weak long-distance NOE is observed at resonance 10 (0.5%). In the case of (iii) there is a significant NOE at resonance 9 (1.8%) and a much smaller NOE at signal 8 (0.5%), but no NOE at any carbonyl in the $Os(CO)_2(PPh_3)$ group. This is inconsistent with structure D. There are no detectable NOE's in the case of (iv). These observed NOE's are consistent with the C···H distances obtained from the crystal structure of **2** (see Table S5, supplementary material).

Chart II

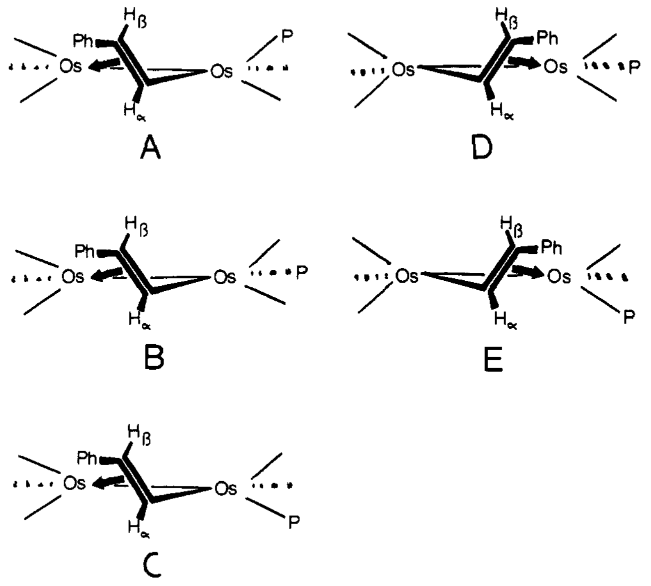

Structures A and B for isomer **1a** are consistent with the NOE results. Although structure B cannot be ruled out categorically, the combined evidence is strongly in favor of structure A. We note that (i) the ^{31}P chemical shift in **1a** and the ^{31}P and ^{187}Os couplings to the carbonyls in the $Os(CO)_2(PPh_3)$ group in **1a** are very similar to those associated with P(1) in complex **2**, implying that this group adopts an identical configuration in both compounds, and (ii) there is no detectable ^{31}P coupling to the vinyl ligand (for either ^1H or ^{13}C signals), which might be expected if it were in a trans geometry. In addition, the T_1 values of 1.55 (±0.05) and 1.27 (±0.05) s for the ^{31}P signals of **1a** and **1b**, respectively (4.7 T, 193 K), are consistent with the orientation of the vinyl substituent, since the phenyl protons and particularly H_β of the vinyl group are closer to the phosphorus atom in **1b** than in structure A. This argument assumes that ^1H–^{31}P dipolar interactions provide a significant contribution to ^{31}P relaxation. An analysis of the spinning-sideband intensities in the ^{31}P CPMAS spectrum of **2**, by the method of Maricq and Waugh,[29] gave principal components of the shift tensors given in the Experimental Section. The chemical shift anisotropies $\Delta\delta$ for the signals at δ 19.4 and −0.9 are respectively 71.1 and 55.7 ppm. The ^{31}P CPMAS signal for solid **1b** shows no spinning sidebands, which indicates that $\Delta\delta$ must be less than 41 ppm. These values of $\Delta\delta$ are relatively small

---

[29] Maricq, M. M.; Waugh, J. S. *J. Chem. Phys.* **1979**, *70*, 3300.

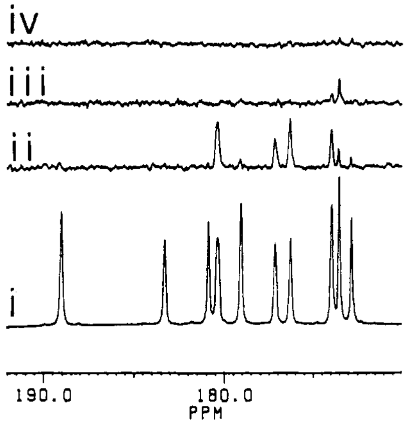

Figure 5. $^{13}C\{^1H\}$ NOE difference spectra for complex 1: (i) control off-resonance spectrum; (ii) irradiation at H_α of isomers **1a** and **1b** minus control spectrum; (iii) irradiation at H_β of isomer **1a** minus control spectrum; (iv) irradiation at H_β of isomer **1b** minus control spectrum.

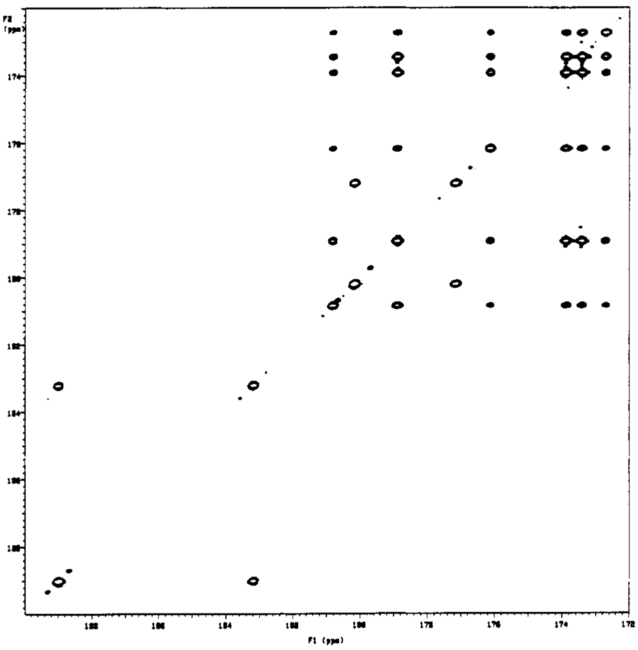

Figure 6. 150.9-MHz ^{13}C EXSY spectrum of complex 1 (mixing time 0.2 s, 273 K). The high signal to noise can be gauged by the appearance of ^{187}Os satellites for resonances 1–4, 6, and 10.

compared with other reported examples[30] and similar to that reported for free PPh_3 (50 ppm).[31] Hence, the relaxation of the ^{31}P nuclei at 4.7T should not be dominated by CSA contributions.[30] The full assignments for **1a**, **1b**, and **2** are shown in Chart I. The exchange between isomers **1a** and **1b** thus corresponds to a simple σ,π-vinyl flip.

In order to examine further the exchange behavior previously reported[15] for 1, ^{13}C EXSY spectra at 150.9 MHz were obtained. Figure 6 shows the spectrum at 273 K (t_m 0.2 s), which indicates there are three independent exchange networks. There is an inter-isomer pairwise exchange between signals 1 and 2, and between signals 4 and 6, due to the σ,π-vinyl flip. The remaining six signals form a third exchange network. If no further exchanges occur, three signals would be expected in the fast-exchange regime, which is indeed observed.[15] The EXSY intensities at mixing times of 0.1, 0.2, and 0.4 s were analyzed by the iterative method of Sales et al.[32] with the two two-site networks and the six-site network treated as two separate problems. Using unconstrained least-squares optimization, the rate constants $k_{1,2}$ = 2.52 (±0.11) s^{-1} and $k_{4,6}$ = 2.37 (±0.10) s^{-1} were obtained, with a goodness of fit (GOF; $\times 10^3$)[33] of 2.5. Since these two site-to-site rate constants are due to the σ,π-vinyl flip, they must be equal to the rate of isomerization k_{isom} of **1a** → **1b** and hence are required to be equal. When this constraint was applied, the rate constant k_{isom} = 2.44 (±0.08) s^{-1} was obtained, with a marginally increased GOF to 2.6.

Table IV. Experimental Exchange Rate Constants (s^{-1}, Esd's in Parentheses) from EXSY Data for Complex 1[a,b]

	3	10	7	8	9	5
3		0.20(9)	0.21(9)	0	0	2.22(10)
10	0.23(12)		0.39(10)	0	2.47(11)	0
7	0.20(12)	0.40(12)		2.42(11)	0	0
8	−0.06(15)	−0.16(16)	2.36(16)		5.28(26)	5.15(26)
9	−0.06(15)	2.49(16)	−0.12(16)	5.66(34)		5.12(26)
5	2.32(15)	0.12(15)	0.19(15)	5.00(32)	4.95(32)	

[a] Bottom left sector of matrix refers to unconstrained optimization and top right sector to zero rate constrained (see text). Interisomer exchange rate constants are given as **1a** → **1b**, due to differing populations $k_{ij} = k_{ji}/K$. [b] For assignment of sites see Chart I.

The exchanges within the six-site network could be satisfactorily analyzed in terms of three independent rate constants. Unconstrained optimization of all 15 rate constants gave the values given in Table IV, with a GOF of 1.03. The rate constants $k_{3,8}$, $k_{3,9}$, $k_{5,7}$, $k_{5,10}$, $k_{7,9}$, and $k_{8,10}$ were either negative or experimentally zero. When these were constrained to be zero, the GOF increased to 1.09, and it became apparent that $k_{7,3} \approx k_{10,3} \approx k_{7,10}$, $k_{5,3} \approx k_{8,7} \approx k_{9,10}$, and $k_{5,8} \approx k_{5,9} \approx k_{9,8}$ (Table IV). When this constraint was applied, the GOF increased to 1.19 and the three independent rate constants $k_{7,3}$ = 0.26 (±0.05) s^{-1}, $k_{5,3}$ = 2.37 (±0.07) s^{-1}, and $k_{5,8}$ = 5.18 (±0.12) s^{-1} were obtained. Since the rate $k_{7,3}$ was small, a zero rate constant was considered, but this gave a significantly worse fit with GOF = 1.52. These three independent exchange rate constants, which provide the best fit to the EXSY data, can readily be interpreted in terms of tripodal rotations in the $Os(CO)_3$ groups of **1a** ($k = 5.18$ s^{-1}) and **1b** ($k = 0.26$ s^{-1}) and a σ,π-vinyl flip which results in isomerization (k_{isom} = 2.37 s^{-1}). The latter mechanism requires a pairwise exchange between the sets (1,2), (4,6), (5,3), (8,7), and (9,10) with the same rate constant, as is indeed observed. The free energies of activation $\Delta G^{\ddagger}{}_{273}$ for the three processes are respectively estimated to be 62.9 (±0.5), 69.7 (±0.7), and 64.7 (±0.5) kJ mol^{-1}.

Conclusions

The magnitudes of $J(^{187}Os-^{13}C)$ in 1 and 2 are virtually identical for carbonyls in related chemical environments and are more useful diagnostic tools than their chemical shifts, which differ by up to 2 ppm. The $^{13}C\{^1H\}$ NOE is relatively easy to measure and should be generally useful in carbonyl assignment where J couplings are of little

---

(30) Randall, L. H.; Carty, A. J. *Inorg. Chem.* **1989**, *28*, 1194 and references therein.

(31) Bemi, L.; Clark, H. C.; Davies, J. A.; Fyfe, C. A.; Wasylishen, R. E. *J. Am. Chem. Soc.* **1982**, *104*, 438.

(32) Beringhelli, T.; D'Alphonso, G.; Molinari, H.; Hawkes, G. E.; Sales, K. D. *J. Magn. Reson.* **1988**, *80*, 45.

(33) The goodness of fit is defined as in ref 32, GOF = $S^{-1}[\Sigma r^2/m]^{1/2}$, where S is the scaling factor, m is the number of data points, and r is the residual between calculated and experimental intensities. The GOF values quoted are *averages* for the three mixing times, to allow for different scaling factors between experiments.

utility. This technique does not appear to have had widespread use, although we note that Hawkes et al.[20] have reported no detectable ^{13}C{^{1}H} NOE in $Os_3(\mu\text{-}H)_2(CO)_{10}$.

Experimental Section

General experimental methods for obtaining and analyzing the 1D magnetization and EXSY spectra were as previously described.[17] ^{31}P NMR spectra were obtained in solution at 81.02 MHz on a Bruker AM200SY spectrometer or in the solid state on a Varian VXR300 at the SERC Solid State NMR service, Durham, U.K. Solution ^{13}C NMR spectra were obtained either at 50.32 MHz on a Bruker AM200SY or at 150.9 MHz on a Varian VXR600S at the SERC Ultra High Field NMR Service, Endinburgh, Scotland. The ^{13}C{^{1}H} NOE experiments were undertaken at low temperature to minimize relayed NOE's due to chemical exchange, though some were observed for 1 (see text). An irradiation time of 4 s at the ^{1}H frequencies (CW power 45 L) was used, with recycle delays of $\sim 5T_1$. EXSY and double quantum filtered (DQF) COSY spectra were acquired in phase-sensitive mode by using 1024 words in the f_2 dimension and 256 words in the f_1 dimension, zero-filled to 1 K. The ^{13}C EXSY spectra for 1 were analyzed by the iterative method of Sales et al.[32] For the ^{31}P CPMAS spectra, principal components of the chemical shift tensors are defined as $|\sigma_{33} - \sigma_{iso}| > |\sigma_{11} - \sigma_{iso}| > |\sigma_{22} - \sigma_{iso}|$ and the chemical shift anisotropy as $\sigma_{33} - \sigma_{iso}$, with $\sigma_{iso} = {}^{1}/_{3}(\sigma_{33} + \sigma_{22} + \sigma_{11})$. ^{13}CO-enriched samples of complexes 1 and 2 were prepared as previously described.[15] The level of enrichmant was ~65–70%, as judged by the isotopomer populations.

^{31}P NMR Data. Complex 1 (CD_2Cl_2, 263 K): δ 17.5 [s, P(**1a**), $^{1}J(^{187}Os\text{-}P)$ = 254 Hz, $^{2}J(^{187}Os\text{-}P)$ = 54 Hz], −0.8 [s, P(**1b**), $^{1}J(^{187}Os\text{-}P)$ = 240 Hz, $^{2}J(^{187}Os\text{-}P)$ = 49 Hz]; CPMAS, ambient temperature, spinning rate 5040 Hz; δ(iso) −3.3, no visible spinning sidebands. Complex 2 ($CDCl_2$, 265 K): δ 15.2 [d, P(1), J(P–P) = 8 Hz, $^{1}J(^{187}Os\text{-}P)$ = 256 Hz, $^{2}J(^{187}Os\text{-}P)$ = 54 Hz], −1.8 [d, P(2), J(P–P) = 8, $^{1}J(^{187}Os\text{-}P)$ = 248, $^{2}J(^{187}Os\text{-}P)$ = 48 Hz]; CPMAS, ambient temperature, spinning rate 3260, δ(iso) 19.4 chemical shift tensors ($\sigma_{11} = -36$, $\sigma_{22} = 4$, $\sigma_{33} = 90.5$), δ(iso) −0.9 chemical shift tensors ($\sigma_{11} = -42$, $\sigma_{22} = -15$, $\sigma_{33} = 54$).

Crystal Structure Determination. Details of data collection procedures and structure refinement are given in Table V. Complex 2 was obtained as bright yellow prisms, suitable for diffraction studies, from CD_2Cl_2. Data were collected on an Enraf-Nonius Turbo-CAD4 diffractometer, running under the CAD4 Express software, with graphite-monochromated X-radiation (λ = 0.710 69 Å). Unit cell parameters were determined by refinement of the setting angles ($\theta \geq 18°$) of 25 reflections. Standard reflections were measured every 2 h during data collection, and no significant variations in intensity were noted. Lorentz–polarization and absorption (DIFABS[34]) corrections were applied. The systematic absences uniquely indicated the centrosymmetric space group $P2_1/c$. The structure was solved by heavy-atom methods for the two Os atoms and by subsequent electron density difference syntheses for the remaining atoms. All non-hydrogen atoms were allowed anisotropic thermal motion. Phenyl hydrogen atoms were included at calculated positions with C–H = 1.0 Å. The two vinylic hydrogen positions were obtained from difference maps, but their positional parameters were allowed to ride on their attached C atom during refinement. Isotropic thermal parameters for all H atoms were fixed at 0.08 Å^2. The phenyl groups were refined as rigid groups with idealized geometry (C–C = 1.395 Å). Refinement was by full-matrix least squares, but due to matrix size limitations the parameters were divided into two blocks of 296 and 179 parameters, and each block was refined separately. The function minimized was $\Sigma w(|F_o| - |F_c|)^2$ with the weighting scheme $w = [\sigma^2(F_o)]^{-1}$ used and judged satisfactory. $\sigma(F_o)$ was estimated from counting statistics. Neutral atom scattering factors were taken from ref 35 with corrections for anomalous dispersion. All calculations were carried out on a MicroVAX 3600 computer using the Glasgow GX suite of programs.[36]

Table V. Experimental Data for the Crystallographic Study

compd formula	$C_{48}H_{37}BrO_4Os_2P_2$
M_r	1200.1
space group	$P2_1/c$ (No. 14; C_{2h}^5)
cryst syst	monoclinic
a/Å	14.256(1)
b/Å	11.650(1)
c/Å	25.841(2)
β/deg	90.243(6)
V/Å^3	4291.9(5)
Z	4
D_{calcd}/g cm^{-3}	1.86
F(000)	2296
μ(Mo Kα)/cm^{-1}	69.6
T/K	298
scan mode	$\theta/2\theta$
θ range/deg	$2 < \theta < 26$
cryst size/mm	0.3 × 0.23 × 0.05
range of transmission coeff cor	0.82–1.29
no. of data collcd	10 072
no. of unique data	8386
hkl range	−17 to +17; 0 to 14; −31 to 0
R_{merge}	0.030
std rflns	170; 6,0,10; $\bar{4},\bar{1}$,13
observability criterion n ($I > n\sigma(I)$)	2
no. of data in refinement	6231
no. of refined params	179/296
final R	0.030
final R_w	0.032
goodness of fit S	1.26
largest remaining feature in electron dens map/e Å^{-3}	+0.74 (max), −0.71 (min)
shift/esd in last cycle	0.11 (max), 0.009 (av)

Acknowledgment. Dr. D. Apperley at the SERC Solid State NMR service, Durham, U.K., is gratefully thanked for obtaining the ^{31}P CPMAS and exchange spectra, and Drs. D. Reed and I. Sadler at the SERC Ultra High Field NMR service are thanked for obtaining 150.9-MHz ^{13}C spectra of 1. Dr. K. D. Sales is also thanked for supplying the program to analyzed EXSY intensities.

Note Added in Proof. Further solid state EXSY experiments on complex 2 at low temperatures have shown that there is no detectable chemical exchange.

Supplementary Material Available: Tables of anisotropic thermal parameters, calculated hydrogen positional parameters, all bond lengths and angles, and selected nonbonding distances (10 pages). Ordering information is given on any masthead page. Tables of observed and calculated structure factors are available from the authors (L.J.F.) on request.

OM920825K

---

(34) Walker, N.; Stuart, D. *Acta Crystallogr., Sect. A: Found. Crystallogr.* **1983**, *A39*, 158.

(35) *International Tables for X-Ray Crystallography*; Kynoch: Birmingham, U.K., 1974; Vol. 4.

(36) Mallinson, P.; Muir, K. W. *J. Appl. Crystallogr.* **1985**, *18*, 51.